

This is a repository copy of *Restoring interlayer Josephson coupling in La_{1.885}Ba_{0.115}CuO₄ by charge transfer melting of stripe order.*

White Rose Research Online URL for this paper:
<https://eprints.whiterose.ac.uk/id/eprint/103330/>

Version: Accepted Version

Article:

Khanna, V., Mankowsky, R., Petrich, M. et al. (10 more authors) (2016) Restoring interlayer Josephson coupling in La_{1.885}Ba_{0.115}CuO₄ by charge transfer melting of stripe order. *Physical Review B*. 224522. pp. 1-5. ISSN 2469-9969

<https://doi.org/10.1103/PhysRevB.93.224522>

Reuse

Items deposited in White Rose Research Online are protected by copyright, with all rights reserved unless indicated otherwise. They may be downloaded and/or printed for private study, or other acts as permitted by national copyright laws. The publisher or other rights holders may allow further reproduction and re-use of the full text version. This is indicated by the licence information on the White Rose Research Online record for the item.

Takedown

If you consider content in White Rose Research Online to be in breach of UK law, please notify us by emailing eprints@whiterose.ac.uk including the URL of the record and the reason for the withdrawal request.

Restoring Interlayer Josephson Coupling in $\text{La}_{1.885}\text{Ba}_{0.115}\text{CuO}_4$ by Charge Transfer Melting of Stripe Order

V. Khanna,^{1,2,3} R. Mankowsky,^{2,4} M. Petrich,^{2,4} H. Bromberger,^{2,4} S. A. Cavill,^{1,5} E. Möhr-Vorobeva,³ D. Nicoletti,^{2,4} Y. Laplace,^{2,4} G. D. Gu,⁶ J. P. Hill,⁶ M. Först,^{2,4} A. Cavalleri,^{2,3,4,*} and S. S. Dhesi^{1,†}

¹*Diamond Light Source, Chilton, Didcot, OX11 0DE, United Kingdom*

²*Max Planck Institute for the Structure and Dynamics of Matter, 22761 Hamburg, Germany*

³*Department of Physics, Clarendon Laboratory, University of Oxford, Oxford, OX1 3PU, United Kingdom*

⁴*Centre for Free Electron Laser Science, 22761 Hamburg, Germany*

⁵*Department of Physics, University of York, Heslington, York, YO10 5DD, United Kingdom*

⁶*Condensed Matter Physics and Materials Science Department, Brookhaven National Laboratory, Upton, NY, United States*

(Dated: May 3, 2016)

We show that disruption of charge-density-wave (stripe) order by charge transfer excitation, enhances the superconducting phase rigidity in $\text{La}_{1.885}\text{Ba}_{0.115}\text{CuO}_4$ (LBCO). Time-Resolved Resonant Soft X-Ray Diffraction demonstrates that charge order melting is prompt following near-infrared photoexcitation whereas the crystal structure remains intact for moderate fluences. THz time-domain spectroscopy reveals that, for the first 2ps following photoexcitation, a new Josephson Plasma Resonance edge, at higher frequency with respect to the equilibrium edge, is induced indicating enhanced superconducting interlayer coupling. The fluence dependence of the charge-order melting and the enhanced superconducting interlayer coupling are correlated with a saturation limit of $\sim 0.5\text{mJ}/\text{cm}^2$. Using a combination of x-ray and optical spectroscopies we establish a hierarchy of timescales between enhanced superconductivity, melting of charge order and rearrangement of the crystal structure.

The interplay between superconductivity and broken electronic symmetries has emerged as a central theme in cuprate physics with increasing reports of charge order in several materials [1–10]. This body of work has led to a growing realization that understanding competing orders may be key to developing high- T_C superconductivity further. An early example of electronic order competing with superconductivity is that of charge and spin (stripe) ordering [1, 11] in underdoped $\text{La}_{2-x}\text{Ba}_x\text{CuO}_4$, where holes doped into the CuO_2 planes order along domain walls, separating regions of antiphased antiferromagnetic spin ordering, below $T \simeq 42\text{K}$. Concomitantly, the crystal structure distorts into a low-temperature tetragonal (LTT) phase which is assumed to align the hole-rich domain walls along the Cu-O-Cu bond direction with a doping dependent stripe modulation [12–14]. The emergence of superconductivity from this stripe phase for $0.09 \lesssim x \lesssim 0.16$ follows a peculiar double-dome phase boundary [15], with the superconducting transition temperature, T_C , greatly suppressed for $x = 1/8$.

A first step in disentangling the hierarchy of cause and effect demonstrated that stripe ordering persists in the absence of the LTT distortion [16, 17]. In a similar fashion mid-IR light has also been used to induce lattice distortions in $\text{La}_{1.875}\text{Ba}_{0.125}\text{CuO}_4$ revealing that the LTT distortion and stripe ordering evolve as distinct non-equilibrium phases with different timescales [18]. More recent work, argues that pair-density waves in the CuO_2 planes completely suppress Josephson coupling between neighboring planes [19, 20]. The loss of interlayer coupling is, however, predicted to be highly sensitive to topo-

logical defects resulting in a complex phase diagram with the emergence of new and novel superconducting phases with increasing defect density [21].

Here, we reveal how puncturing stripe order, with charge transfer defects introduced by near-infrared optical pulses, can dynamically enhance the superconducting order at the expense of stripe order. Specifically, we combine photoexcitation, Time-Resolved Resonant Soft X-ray Diffraction (TR-RSX) and THz time-domain spectroscopy to demonstrate that ultrafast disruption of the stripe ordered phase promptly enhances interlayer Josephson coupling in $\text{La}_{1.885}\text{Ba}_{0.115}\text{CuO}_4$ (LBCO). Furthermore, we show that the fluence dependence of the enhanced interlayer Josephson coupling follows closely that of the stripe order melting and not that of lattice rearrangement.

We studied LBCO, for which bulk superconductivity develops at $T_C \simeq 13\text{K}$, spin-ordering at $T_{SO} \simeq 42\text{K}$ and charge ordering along with the LTT distortion at $T_{CO} \simeq T_{LTT} \simeq 53\text{K}$ [11]. Stripe ordering in LBCO is described using a charge-density wave with incommensurate wave vector $(0.23 \ 0 \ 0.65)$ [22]. The LTT structural distortion involves a buckling of the Cu-O-Cu bonds in the CuO_2 planes and a tilting of the CuO_6 octahedra which allows the $(0 \ 0 \ 1)$ reflection [12]. The intensities of the $(0.23 \ 0 \ 0.65)$ and $(0 \ 0 \ 1)$ diffraction peaks are therefore direct probes of the degree of stripe ordering and LTT distortion.

Single crystals of LBCO were grown using the traveling-solvent-floating zone method [11]. Two samples from the same batch were used; one was cleaved along the ab sur-

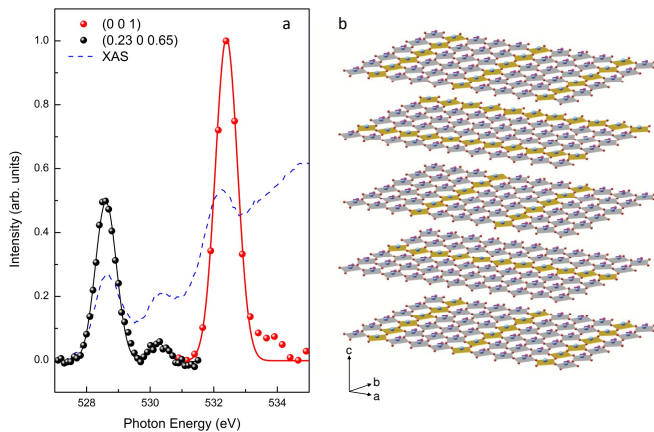


FIG. 1. (Color online) (a) XAS spectrum for LBCO over the O K -edge (dashed blue line) along with the (0.23 0 0.65) charge-ordering diffraction peak (black circles) and (001) LTT distortion diffraction peak (red circles). The lines represent Lorentzian fits to the data. The (0.23 0 0.65) peak has been scaled up by a factor of 3000. (b) Schematic of the stripe ordering (yellow polygons) in the CuO_2 planes.

face for TR-RSX, the other cut and polished to give an ac surface for THz spectroscopy. All measurements were carried out in the superconducting state ($T \approx 5\text{K}$). The 1.55eV (800nm) pump pulses used to photoexcite the sample were σ -polarized, parallel to the Cu-O-Cu bond direction. The penetration depth at 1.55 eV and ~ 530 eV, estimated from LBCO equilibrium optical properties, is similar (~ 200 nm) [23, 24], so that a homogeneous photoexcited volume was probed. The 1.55eV pump pulses from a Ti:Sa amplifier running at 22 KHz were focused down to a spot size of $\sim 200\mu\text{m}$ (FWHM) onto the sample, whilst the X-ray spot size was $\sim 100\mu\text{m}$. The diffraction peak intensities were measured using a gated micro-channel plate, which was insensitive to the 1.55eV pump.

Figure 1 shows the energy dependence of the (0.23 0 0.65) stripe and (0 0 1) structural diffraction peaks as well as the x-ray absorption spectroscopy (XAS) spectrum across the O K -edge recorded at $T=5\text{K}$. The resonances at 528.6 eV, along with the weak shoulder at 530.2 eV, correspond to transitions into the states associated with the doped holes and the upper Hubbard band [25]. The (0 0 1) diffraction peak has a strong resonance at the O K -edge, centered at 532.4 eV corresponding to resonant transitions into La-O hybridized states [12].

We first discuss the TR-RSX results. The temporal evolution of both the stripe and LTT phase after photoexcitation was investigated using ultrafast changes in the (0.23 0 0.65) and (0 0 1) diffraction peaks relative to the fluorescence background. Figure 2 shows the change in diffraction peak intensities ($\Delta I_\tau / I_0$) as a function of time delay (τ), for an excitation fluence of 1.6 mJ/cm^2 . The results were recorded with the storage ring operating in low- α mode, for which the longitudinal width of

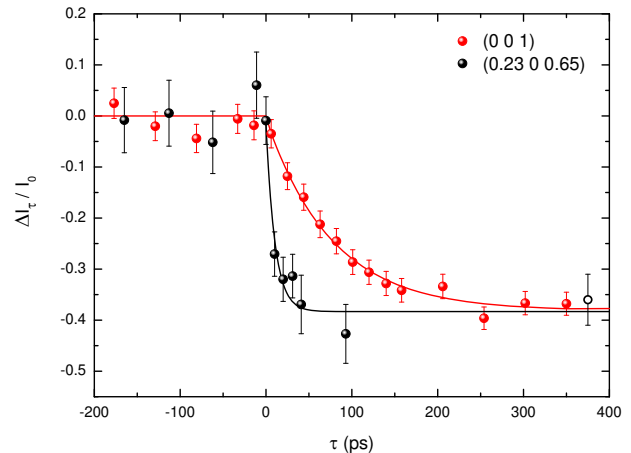


FIG. 2. (Color online) Intensity changes in the (0.23 0 0.65) charge-ordering diffraction peak (solid black circles) and (001) LTT distortion diffraction peak (solid red circles) following near-infrared photoexcitation using a pump fluence of 1.6 mJ/cm^2 . The data were measured in low- α mode with an X-ray pulse width of $\sim 7\text{ps}$ (FWHM) except for the open circle which represents the change in intensity of the (0.23 0 0.65) diffraction peak for $\tau=375\text{ps}$ recorded in hybrid mode with an X-ray pulse width of $\sim 60\text{ps}$ (FWHM). The solid lines represent fits to the data using an exponential function.

the electron bunch was compressed to give a temporal resolution of $\sim 7\text{ps}$ at the expense of photon flux.

For the same excitation fluence, both the (0.23 0 0.65) and (0 0 1) peaks are reduced in intensity by $\sim 40\%$. However, the temporal response after photoexcitation is different. A fit to the stripe peak data (Fig. 2, black line) gives a time constant of 10 ± 3 ps and is limited by the X-ray pulse width in the low- α mode of operation. However, the decay in the stripe peak is likely to be prompt, occurring within only a few hundred femtoseconds of photoexcitation [18]. The (0 0 1) peak, on the other hand, is observed to decrease over a much slower timescale with an exponential fit (Fig. 2, red line) yielding a time constant of 77 ± 7 ps. We note here that the different responses of the two peaks precludes loss of intensity from sample heating from the laser pulses since $T_{CO} \approx T_{LTT}$. Previous studies using mid-infrared excitation of in-plane stretching modes have shown enhancement of interlayer coupling in a number of cuprates [26, 27], but little is known regarding the fate of the charge ordered phase in the non-equilibrium state [18, 28]. Figure 2, demonstrates that photoexcitation using near-infrared 1.55eV pulses creates a charge transfer non-equilibrium phase in which the LTT distortion remains intact, but the stripe ordering is strongly suppressed. This then gives a unique system with which to explore the emerging dynamics of superconductivity once stripe order is disrupted.

The photoinduced dynamics of the superconducting condensate were measured using transient reflectivity at THz frequencies. The sample was excited under the same

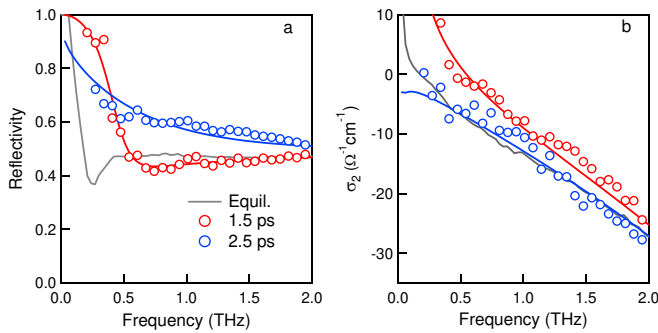


FIG. 3. (Color online) (a) Normal-incidence reflectivity and (b) imaginary conductivity (σ_2) from LBCO measured with THz time-domain spectroscopy 1.5 ps (red circles) and 2.5 ps (blue circles) after near-infrared optical excitation. The same quantities measured at equilibrium are displayed as gray lines. Red and blue lines are fits to the data performed with a superconducting and Drude model, respectively.

conditions used in the TR-RSX work with near-infrared 1.55eV laser pulses. The weak interlayer superconducting coupling of LBCO results in an equilibrium Josephson Plasmon Resonance (JPR) at $\sim 0.2\text{THz}$ [29, 30] in the c -axis reflectivity and is shown as the gray line in Fig. 3(a). Superconducting transport is also observed as a small low-frequency divergence of the imaginary part of the conductivity (σ_2) and is shown as the grey line in Fig. 3(b).

The transient optical properties of the photoexcited LBCO were measured in the 0.15-2 THz spectral range for different pump fluences as a function of τ , with a time resolution of $\sim 350\text{fs}$, determined by the inverse bandwidth of the THz probe pulse. The mismatch between the penetration depth of the near-infrared 1.55eV pump ($\sim 0.1\mu\text{m}$) and that of the THz probe ($\sim 50\text{-}500\mu\text{m}$) was taken into account using a multilayer model [27, 31]. The c -axis transient reflectivity and σ_2 spectra, measured 1.5ps after photoexcitation, are shown in Fig. 3 (red circles) for a pump fluence of $1.6\text{mJ}/\text{cm}^2$. The JPR displays a prompt blue-shift from $\sim 0.25\text{THz}$ to $\sim 0.5\text{THz}$ (Fig. 3(a), red circles). Correspondingly, an enhancement of σ_2 is indicative of an increase in interlayer Josephson coupling (Fig. 3(b), red circles). At $\tau=2.5\text{ps}$ we observe a relaxation to a state in which coherence is reduced, characterized by a broader edge in reflectivity (Fig. 3(a), blue circles) and the absence of a divergence in σ_2 (Fig. 3(b), blue circles). In analogy with previous optical results for LBCO after photoexcitation perpendicular to the CuO_2 planes [30, 32], the transient spectra could be fitted assuming a superconducting model for $\tau=1.5\text{ps}$ (Fig. 3, red lines), while in the relaxed state a Drude model with a finite carrier scattering time in the picosecond range had to be employed (Fig. 3, blue lines). Notably, in the case of in-plane pumping explored here, the blue-shift of the JPR is less marked and the relaxation to the incoherent state is faster with respect to the case of c -axis

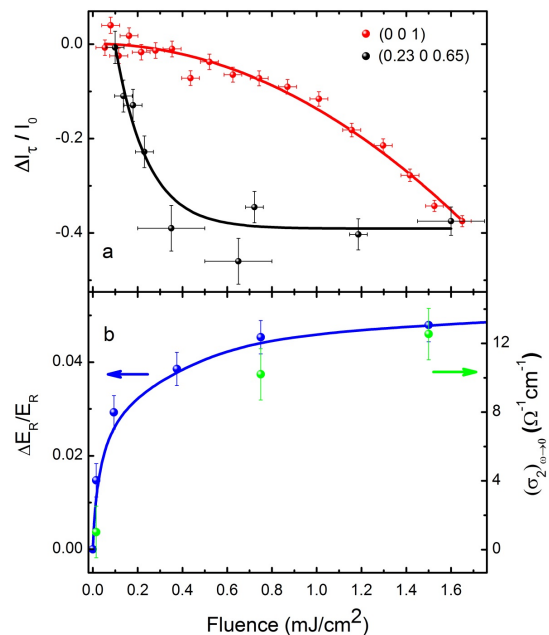


FIG. 4. (Color online) (a) Fluence dependence of the (0.23 0 0.65) charge-ordering diffraction peak (solid black circles) and (001) LTT distortion diffraction peak (solid red circles) intensity after photoexcitation with $\tau=350\text{ps}$. The error in the fluence indicates the uncertainty in the pump beam diameter at the sample position. The red line shows a quadratic fit whereas the black line shows an exponential fit to the data. (b) Changes in the electric field, $\Delta E_R / E_R$ (solid blue circles) and $(\sigma_2)_{\omega \rightarrow 0}$ (solid green circles) as a function of fluence (Frequency = 0.2THz , $\tau = 1.5\text{ps}$). The blue line shows a fit using an exponential function.

pumping [30], most likely due to stronger coupling to quasiparticle excitation in the planes. The enhancement of the superconducting phase using charge transfer excitation is surprising given that the process generates high energy electrons that relax via the emission of phonons which subsequently destroy the Cooper pairs [33–35]. For LBCO the disruption of interlayer superconductivity due to pair-density waves [20] is presumably removed following charge transfer leading to an enhancement of the superconducting phase before its destruction from the creation of quasiparticles.

The measurement of both TR-RSX and THz time-domain reflectivity, under the same near-infrared excitation conditions, allows the first direct comparison of the time scales involved in the dynamics. The interlayer coupling enhancement, which develops in $\sim 1\text{ps}$ following photoexcitation, is strongly connected with the stripe order melting shown in Fig. 2. On the other hand, the lattice dynamics start to develop on considerably longer timescales ($>10\text{ps}$).

Further insights regarding the enhanced interlayer coupling and the disruption of stripe order can be retrieved from the pump fluence dependence of the intensities mea-

sure using TR-RSX and THz spectroscopy. Figure 4(a) shows $\Delta I_{\tau}/I_0$ for the stripe and LTT distortion diffraction peaks as a function of fluence for $\tau=350$ ps. The results were recorded with the storage ring operating in hybrid mode with a temporal resolution of ~ 60 ps. This establishes that at ~ 0.5 mJ/cm² the melting of the stripe ordering saturates whereas the LTT distortion remains largely intact which should remain the case for the shortest picosecond timescales inaccessible for synchrotron based TR-RSX. These changes can then be compared with the fluence-dependent Josephson interlayer coupling enhancement (Fig. 4b), estimated by the increase in the low-frequency limit of the imaginary part of the conductivity $(\sigma_2)_{\omega \rightarrow 0}$ and by the change in the reflected electric field $(\Delta E_R/E_R)$ at the peak of the response ($\tau=1.5$ ps). These results confirm the causal link between stripe melting and superconductivity enhancement, as both the (0.23 0 0.65) diffraction peak and the σ_2 response show a clear saturation at ~ 0.5 mJ/cm² fluence, which is not present for the (0 0 1) peak.

The results show that charge transfer destruction of stripe order enhances interlayer superconducting coupling in La_{1.885}Ba_{0.115}CuO₄. The fluence dependence of the charge transfer collapse of stripe order along with the concomitant emergence of an improved superconducting phase should encourage further work to reveal the nature of the charge transfer process [36]. Systematic studies of the conditions required to depress stripe order using charge transfer may become effective for high-speed devices in which the electrical, optical and magnetic properties of highly-correlated materials can be modified using near-infrared light.

We thank Diamond Light Source for the provision of beamtime under proposal numbers SI-7497, SI-7942 and SI-8207. The research leading to these results has received funding from the European Research Council under the European Union's Seventh Framework Programme (FP7/2007-2013) / ERC Grant Agreement n 319286 (Q-MAC). Work at Brookhaven was supported by the Office of Basic Energy Sciences (BES), Division of Materials Sciences and Engineering, U.S. Department of Energy (DOE), through Contract No. DE-SC00112704.

* Electronic mail: andrea.cavalleri@mpsd.mpg.de

† Electronic mail: dhesi@diamond.co.uk

- [1] J. M. Tranquada, B. J. Sternlieb, J. D. Axe, Y. Nakamura, and S. Uchida, *Nature (London)* **105**, 087203 (1995)
- [2] T. Wu, H. Mayaffre, S. Krämer, M. Horvatić, C. Berthier, W. N. Hardy, R. Liang, D. A. Bonn, and M. H. Julien, *Nature (London)* **477**, 191 (2011)
- [3] G. Ghiringhelli, M. Le Tacon, M. Minola, S. Blanco-Canosa, C. Mazzoli, N. B. Brookes, G. M. De Luca, A. Frano, D. G. Hawthorn, F. He, T. Loew, M. Moretti Sala, D. C. Peets, M. Salluzzo, E. Schierle, R. Sutarto, G. A. Sawatzky, E. Weschke, B. Keimer, and L. Braicovich, *Science* **337**, 821 (2012)
- [4] J. Chang, E. Blackburn, A. T. Holmes, N. B. Christensen, J. Larsen, J. Mesot, R. Liang, D. A. Bonn, W. N. Hardy, A. Watenphul, M. v. Zimmermann, E. M. Forgan, and S. M. Hayden, *Nature Phys.* **8**, 871 (2012)
- [5] R. Comin, A. Frano, M. M. Yee, Y. Yoshida, H. Eisaki, E. Schierle, E. Weschke, R. Sutarto, F. He, A. Soumyanarayanan, Y. He, M. Le Tacon, I. S. Elfimov, J. E. Hoffman, G. A. Sawatzky, B. Keimer, and A. Damascelli, *Science* **343**, 390 (2014)
- [6] E. H. da Silva Neto, P. Aynajian, A. Frano, R. Comin, E. Schierle, E. Weschke, A. Gyenis, J. Wen, J. Schneeloch, Z. Xu, S. Ono, G. Gu, M. Le Tacon, and A. Yazdani, *Science* **343**, 393 (2014)
- [7] W. Tabis, Y. Li, M. Le Tacon, L. Braicovich, A. Kreyssig, M. Minola, G. Dellea, E. Weschke, M. J. Veit, M. Ramazanoglu, A. I. Goldman, T. Schmitt, G. Ghiringhelli, N. Barišić, M. K. Chan, C. J. Dorow, G. Yu, X. Zhao, B. Keimer, and M. Greven, *Nat. Commun.* **5**, 5875 (2014)
- [8] R. Comin, R. Sutarto, E. H. da Silva Neto, L. Chauviere, R. Liang, W. N. Hardy, D. A. Bonn, F. He, G. A. Sawatzky, and A. Damascelli, *Science* **347**, 1335 (2015)
- [9] L. E. Hayward, D. G. Hawthorn, R. G. Malko, and S. Sachdev, *Science* **343**, 1336 (2014)
- [10] K. Fujita, C.-K. Kim, J. Lee, M. H. Hamidian, I. A. Firmo, S. Mukhopadhyay, H. Eisaki, M. J. Lawler, E.-A. Kim, and J. C. Davis, *Science* **344**, 612 (2014)
- [11] M. Hücker, M. v. Zimmermann, G. D. Gu, Z. J. Xu, J. S. Wen, G. Xu, H. J. Kang, A. Zheludev, and J. M. Tranquada, *Phys. Rev. B* **83**, 104506 (2011)
- [12] J. Fink, V. Soltwisch, J. Geck, E. Schierle, E. Weschke, and B. Büchner, *Phys. Rev. B* **83**, 092503 (2011)
- [13] M. K. Crawford, R. L. Harlow, E. M. McCarron, W. E. Farneth, J. D. Axe, H. Chou, and Q. Huang, *Phys. Rev. B* **44**, 7749 (1991)
- [14] T. Suzuki and T. Fujita, *Physica C* **159**, 111 (1989)
- [15] A. R. Moodenbaugh, Y. Xu, M. Suenaga, T. J. Folkerts, and R. N. Shelton, *Phys. Rev. B* **38**, 4596 (1988)
- [16] M. Hücker, M. v. Zimmermann, M. Debessai, J. S. Schilling, J. M. Tranquada, and G. G. D., *Phys. Rev. Lett* **104**, 057004 (2010)
- [17] V. Thampy, M. P. M. Dean, N. B. Christensen, L. Steinke, Z. Islam, M. Oda, M. Ido, N. Momono, S. B. Wilkins, and J. P. Hill, *Phys. Rev. B* **90**, 100510(R) (2014)
- [18] M. Först, R. I. Tobey, H. Bromberger, S. B. Wilkins, V. Khanna, A. D. Caviglia, Y.-D. Chuang, W. S. Lee, W. F. Schlotter, J. J. Turner, M. P. Minitti, O. Krupin, Z. J. Xu, J. S. Wen, G. D. Gu, S. S. Dhesi, A. Cavalleri, and J. P. Hill, *Phys. Rev. Lett.* **112**, 157002 (2014)
- [19] Q. Li, M. Hücker, G. D. Gu, A. M. Tsvelik, and J. M. Tranquada, *Phys. Rev. Lett.* **99**, 067001 (2007)
- [20] E. Berg, E. Fradkin, E.-A. Kim, S. A. Kivelson, V. Oganesyan, J. M. Tranquada, and S. C. Zhang, *Phys. Rev. Lett.* **99**, 127003 (2007)
- [21] E. Berg, E. Fradkin, and S. A. Kivelson, *Nature Phys.* **5**, 830 (2009)
- [22] P. Abbamonte, A. Rusydi, S. Smadici, G. D. Gu, G. A. Sawatzky, and D. L. Feng, *Nature Phys.* **1**, 155 (2005)
- [23] C. C. Homes, M. Hücker, Q. Li, Z. J. Xu, J. S. Wen, G. D. Gu, and J. M. Tranquada, *Phys. Rev. B* **85**, 134510

- (2012)
- [24] Y.-H. Kao, H. Kwok, and D. T. Shaw, *Superconductivity and Applications*, edited by Y.-H. Kao, H. Kwok, and D. T. Shaw (Springer, 1989) p. 281
- [25] J. Fink, E. Schierle, E. Weschke, J. Geck, D. Hawthorn, V. Soltwisch, H. Wadati, H.-H. Wu, H. A. Dürr, N. Wizenant, B. Büchner, and G. A. Swatzky, *Phys. Rev. B* **79**, 100502 (2009)
- [26] D. Fausti, R. I. Tobey, N. Dean, S. Kaiser, A. Dienst, M. C. Hoffmann, S. Pyon, T. Takayama, H. Takagi, and A. Cavalleri, *Science* **331**, 189 (2011)
- [27] W. Hu, S. Kaiser, D. Nicoletti, C. R. Hunt, I. Gierz, M. C. Hoffmann, M. Le Tacon, T. Loew, B. Keimer, and A. Cavalleri, *Nat. Mater.* **13**, 705 (2014)
- [28] M. Först, A. Frano, S. Kaiser, R. Mankowsky, C. R. Hunt, J. J. Turner, G. L. Dakovski, M. P. Minitti, J. Robinson, T. Loew, M. Le Tacon, B. Keimer, J. P. Hill, A. Cavalleri, and S. S. Dhesi, *Phys. Rev. B* **90**, 184514 (2014)
- [29] The THz-frequency reflectivity ratios measured above and below T_c were combined with the broadband (up to $10,000\text{ cm}^{-1}$) reflectivity. By applying Kramers-Kronig transformations, a full set of equilibrium optical properties at $T=5\text{K}$ could be determined
- [30] D. Nicoletti, E. Casandruc, Y. Laplace, V. Khanna, C. R. Hunt, S. Kaiser, S. S. Dhesi, G. D. Gu, J. P. Hill, and A. Cavalleri, *Phys. Rev. B* **90**, 100503 (2014)
- [31] The penetration depth mismatch was taken into account by modelling the response of the system as that of a homogeneously photo-excited thin layer on top of an unperturbed bulk which retains the equilibrium optical properties. By calculating the coupled Fresnel equations of such a multi-layer, the transient optical response of the photoexcited layer could be derived.
- [32] E. Casandruc, D. Nicoletti, S. Rajasekaran, Y. Laplace, V. Khanna, G. D. Gu, J. P. Hill, and A. Cavalleri, *Phys. Rev. B* **91**, 174502 (2015)
- [33] P. Kusar, V. V. Kabanov, J. Demsar, T. Mertelj, S. Sugai, and D. Mihailovic, *Phys. Rev. Lett.* **101**, 227001 (2008)
- [34] C. L. Smallwood, J. P. Hinton, C. Jozwiak, W. Zhang, J. D. Koralek, H. Eisaki, D.-H. Lee, J. Orenstein, and A. Lanzara, *Science* **336**, 1137 (2012)
- [35] R. Cortés, L. Rettig, Y. Yoshida, H. Eisaki, M. Wolf, and U. Bovensiepen, *Phys. Rev. Lett.* **107**, 097002 (2011)
- [36] M. Magnuson, T. Schmitt, V. N. Strocov, J. Schlappa, A. S. Kalabukhov, and L.-C. Duda, *Sci. Rep.* **4:7017**, 1 (2015)